
Since January 2020 Elsevier has created a COVID-19 resource centre with free information in English and Mandarin on the novel coronavirus COVID-19. The COVID-19 resource centre is hosted on Elsevier Connect, the company's public news and information website.

Biosensors and Bioelectronics 171 (2021) 112685

Contents lists available at ScienceDirect

Biosensors and Bioelectronics

journal homepage: http://www.elsevier.com/locate/bios

# One-step rapid quantification of SARS-CoV-2 virus particles via low-cost nanoplasmonic sensors in generic microplate reader and point-of-care device

Liping Huang [a,b,*], Longfei Ding [c], Jun Zhou [d], Shuiliang Chen [e], Fang Chen [e], Chen Zhao [c], Jianqing Xu [c,**], Wenjun Hu [a,***], Jiansong Ji [f,****], Hao Xu [b,*****], Gang L. Liu [a,******]

[a] National Engineering Research Center for Nanomedicine, College of Life Science and Technology, Huazhong University of Science and Technology, 1037 Luo Yu Road, Wuhan, 430074, PR China
[b] Liangzhun (Shanghai) Industrial Co. Ltd, Shanghai, China
[c] Shanghai Public Health Clinical Center, Fudan University, China
[d] Wuhan Xinxin Semiconductor Manufacturing Co. Ltd, Wuhan, China
[e] Taiwan Semiconductor Manufacturing Co., Shanghai, China
[f] Lishui Central Hospital, Zhejiang University, Zhejiang, China

ARTICLE INFO

*Keywords:*
COVID-19
SARS-CoV-2 virus
Nanoplasmonic sensor
Antibody conjugation
Point of care testing

ABSTRACT

The spread of SARS-CoV-2 virus in the ongoing global pandemic has led to infections of millions of people and losses of many lives. The rapid, accurate and convenient SARS-CoV-2 virus detection is crucial for controlling and stopping the pandemic. Diagnosis of patients in the early stage infection are so far limited to viral nucleic acid or antigen detection in human nasopharyngeal swab or saliva samples. Here we developed a method for rapid and direct optical measurement of SARS-CoV-2 virus particles in one step nearly without any sample preparation using a spike protein specific nanoplasmonic resonance sensor. As low as 370 vp/mL were detected in one step within 15 min and the virus concentration can be quantified linearly in the range of 0 to $10^7$ vp/mL. Measurements shown on both generic microplate reader and a handheld smartphone connected device suggest that our low-cost and rapid detection method may be adopted quickly under both regular clinical environment and resource-limited settings.

## 1. Introduction

The ongoing COVID-19 pandemic is caused by the respiratory infections of SARS-CoV-2 (Severe Acute Respiratory Syndrome Coronavirus 2) virus between humans(Lipman et al., 2020; Wang et al., 2020). It is evident that the infection may be effectively reduced and eventually controlled with swift and large-scale testing for early diagnostics(Chen et al., 2020; Loeffelholz and Tang, 2020; Wyllie et al., 2020; Yang et al., 2020). Current testing methods include PCR nucleic acid detection with either thermal cycling or isothermal amplification, serological IgM/IgG antibody testing as well as viral protein detections in nasopharyngeal swap (Baek et al., 2020; Corman et al., 2020; Guan et al., 2004; Liu et al., 2020; Lu et al., 2020; Yan et al., 2020; Younes et al., 2020). The PCR based nucleic acid testing is very sensitive and accurate in early infection diagnostics but it generally requires multiple and lengthy processes including virus lysis, RNA extraction, reverse transcription and amplification and is prone to sample contamination(Ai et al., 2020; Yoon et al., 2020). Serological IgM/IgG antibody testing is a very rapid and potentially point-of-care detection method for epidemiology studies of past viral infections, although not adequate for early diagnosis, since the serological antibody presence will not occur until a couple of weeks after the initial viral infection (Haveri et al., 2020; Sethuraman et al., 2020;

* Corresponding authors. Huazhong University of Science and Technology, 1037 Luo Yu Road, Wuhan, 430074, PR China.
** Corresponding authors. Huazhong University of Science and Technology, 1037 Luo Yu Road, Wuhan, 430074, PR China.
*** Corresponding authors. Huazhong University of Science and Technology, 1037 Luo Yu Road, Wuhan, 430074, PR China.
**** Corresponding authors. Liangzhun (Shanghai) Industrial Co. Ltd, Shanghai, China
***** Corresponding authors. Shanghai Public Health Clinical Center, Fudan University, China
****** Corresponding authors. Zhejiang University, Zhejiang, China
*E-mail addresses:* lphuang@aliyun.com (L. Huang), billxu@kaizzi.com (H. Xu), loganliu@hust.edu.cn (G.L. Liu).

https://doi.org/10.1016/j.bios.2020.112685
Received 2 July 2020; Received in revised form 29 September 2020; Accepted 2 October 2020
Available online 15 October 2020

To et al., 2020). There were some reported and commercially available viral antigen spike (S) or nucleocapsid (N) protein detection assays however they all suffered with very poor accuracy, reliability and sensitivity. Therefore it is a global consensus there is an urgent and tremendous demand for low-cost rapid and reliable SARS-CoV-2 antigen and virus detection which helps to enable timely and affordable point-of-care COVID-19 diagnostics for a very large population.

As the matter of fact, surface plasmon resonance (SPR) sensing is a promising label free and one-step virus detection method and has been used in rapid viral particle detection such as SARS/MERS, H1N1 and H7N9, etc. (Chang et al., 2018; Su et al., 2012; Wang et al., 2006) Once the viral particles are captured by the monoclonal antibody immobilized on the SPR sensor chip surface, the plasmon resonance wavelength or intensity change induced by the virus particle presence can be measured by an optical sensing system(Jackman et al., 2016; Victoria, 2012; Yanik et al., 2010). However conventional SPR testing equipment are bulky and not affordable to most research and clinical institutions especially in developing countries and resources limited settings(Moran et al., 2018; Puiu and Bala, 2016). Therefore the SPR virus detection, although often showed in research labs, rarely becomes a viable method accessible to clinical and point-of-care applications.

Here we report a low-cost nanoplasmonic sensor allowing for one-step rapid detection and quantification of the SARS-CoV-2 pseudovirus (Fig. 1a). The low-cost plasmonic nanocup array sensor chips were made by the method previously reported (Dang et al., 2019; Hu et al., 2019), and this method allows for large-scale manufacturing with high uniformity and repeatability. Owing to the specially designed periodic nanostructures, without any external coupling optics, the plasmon resonance wavelength and intensity change on the virus-capturing sensor surface can be simply observed by transmission light spectroscopy or imaging(Soler et al., 2017; Zhang et al., 2016). Therefore the nanoplasmonic sensor chips can be integrated with microwell plate or microfluidic cuvette, and the measurements are carried out in both ubiquitous generic microplate readers and a low-cost handheld point-of-care testing device(Dang et al., 2019; Hu et al., 2019). The genetically reconstructed pseudovirus for SARS-CoV-2, SARS (Severe Acute Respiratory Syndrome), MERS (Middle East Respiratory Syndrome), and VSV (Vesicular Stomatitis Virus) viruses were produced for testing the device sensitivity and specificity (Hoffmann et al., 2020; Rabaan et al., 2020; Wrapp et al., 2020). With proper antibody functionalization on its surface, the nanoplasmonic sensor is able to detect as low as 370 vp/mL SARS-CoV-2 pseudovirus while showing negligible responses to SARS, MERS and VSV pseudoviruses. SARS-CoV-2 virus concentrations in the range of $10^2$ vp/mL to $10^7$ vp/mL can also be quantified by this assay with simultaneous measurements of diluted standard samples in the same microplate reader. Similar sensing capability are demonstrated by using a low-cost handheld optical equipment controlled by a smartphone App. The ultrasensitive SARS-CoV-2 virus detection and potential early diagnosis of COVID-19 disease become available for point-of-care applications in clinics, roadside triage sites and even home settings.

## 2. Experimental

### 2.1. Materials

Hexylsilane, 6-mercapto-1-hexanol (MCH), 11-mercaptuoudecanoic acid (MUA), 1-ethyl-3-(dimethylaminopropyl) carbodiimide (EDC), N-hydroxysuccinimide (NHS), bovine serum albumin (BSA), ethanolamine and phosphate-buffered saline (PBS) buffer were purchased from Sigma-Aldrich, SARS-COV-2 Antibody-CR3022 (catalog no. CHA005) was purchased from Sanyou Biopharmaceuticals Co., Ltd. SARS-COV-2 RBD-mAbs (GHMA 105–1, GHMA 105–2) was purchased from Goodhere Biological Technology Co., Ltd. Angiotensin-Converting Enzyme 2 (ACE2) Protein (catalog no. 2020T13) was purchased from Shanghai EasyBiotech Co., Ltd.. All chemicals were used as obtained without any

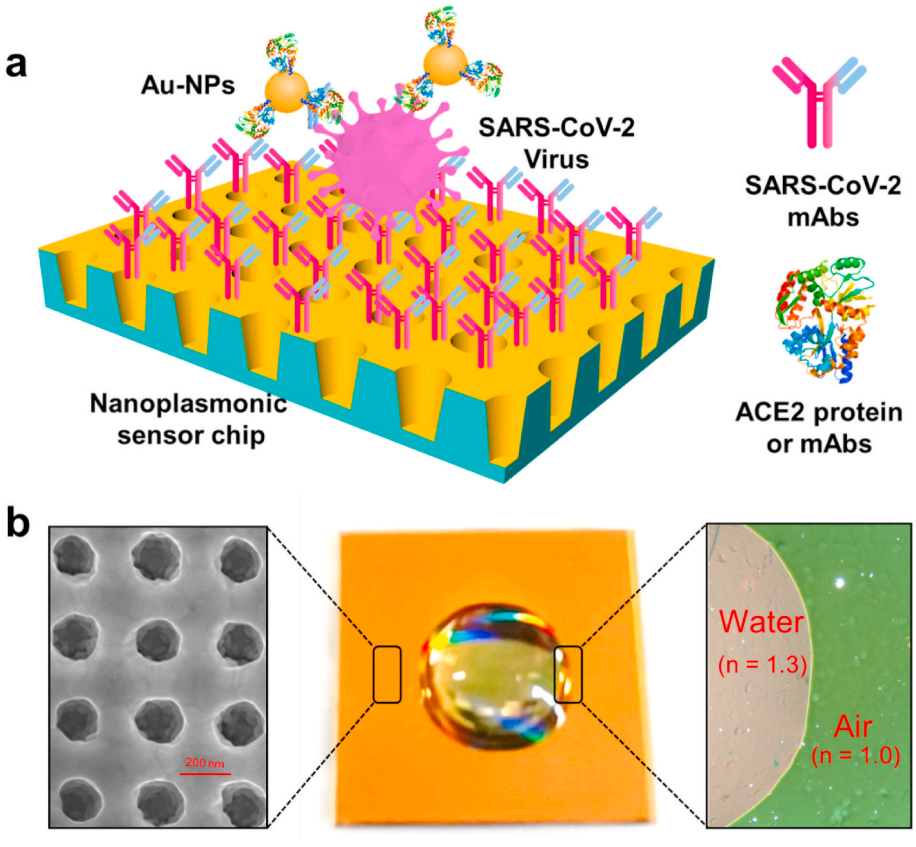


**Fig. 1.** Label-free detection of SARS-CoV-2 pseudovirus with a nanoplasmonic sensor. (a) Schematic diagram of the nanoplasmonic resonance sensor for determination of SARS-CoV-2 pseudovirus concentration. (b) Photograph (Middle) of one piece of Au nanocup array chip with a drop of water on top. Scanning electron microscopy image (Left) shows the replicated nanocup array. Transmission microscopy image (Right) shows that air and water on the device surface exhibit different colors, green and far red pink, respectively.

further purification. The SARS-CoV-2 pseudovirus samples were obtained from Shanghai public health clinical center.

### 2.2. Fabrication process

The nanoplasmonic sensor was fabricated by a replica molding process. The original mold was a tapered nanopillar array (diameter = 220 nm, depth = 500 nm, period = 440 nm) on a silicon wafer made by photolithography and plasma etching. An optical adhesive liquid was evenly spread on the mold and placed on a polyethylene terephthalate (PET) sheet. After 3 min of UV light (105 mW/cm$^2$) irradiation, the PET sheet with the UV polymer layer was peeled off from the mold. Then, 10 nm of titanium (Ti) and 70 nm of gold (Au) were deposited onto the nanocup array in an electron beam evaporator. Later the sheet were cut into small pieces of 1 cm × 1 cm, and glued to an open-bottom 96-well plate or a chip cartridge made by a 3D printer (Object 30 primer™ Stratasys Ltd.).

### 2.3. Surface functionalization

After rinsing the chip integrated microplate wells or cards twice with deionized (DI) water, the chips were incubated in a 10 mM MUA ethanol solution for 0.5 h at room temperature. Clean the chips with 70% ethanol and DI water twice followed by immersion in a mixture of 400 mM EDC and 100 mM NHS for 30 min to activate the chips at room temperature. Next, the chips were rinsed in DI water twice and the SARS-CoV-2 monoclonal antibodies (mAbs) of 12.0 μg/mL (in PBS) were immediately immobilized to the activated chips for 4 h at room temperature. Rinse the chips with PBS and DI water, and afterwards incubate the chips in 60 μg/mL BSA blocking solution and then in 10% ethanolamine solution, and both steps last for 30 min at room temperature. After incubation, functionalized chips were gently rinsed with DI water twice and then stored in a humid atmosphere at 4 °C.

### 2.4. Preparation of gold labeled with ACE2 protein or SARS-CoV-2 mAbs

Au-NPs labeled with ACE2 protein or SARS-CoV-2 mAbs prepared in pH 7.0 Glycine-buffered solution (100 nmol/L) was added drop-wise to 1 mL of 30 nm colloidal Au-NPs solution. The pH of the colloidal Au-NPs solution was adjusted to pH 7.2 by addition of dilute 0.01 M $K_2CO_3$ before adding the ACE2 protein or SARS-CoV-2 mAbs. This was done in as much as the optimum stability of the conjugates is at pH 7.2, and the least content of antibody was 0.023 mg/mL of gold solution. The ACE2 protein or SARS-CoV-2 mAbs was initially incubated with Au-NPs for 30 min. After incubation, 10 μL of Tris-HCl 1 × with 1% BSA blocking solution was added to the gold labeled solution for 10 min. The Au-NPs suspension was then centrifuged at 8000 rpm for 30 min. Centrifugation and resuspension steps were repeated 3 times. At the final resuspension step, Au-NPs precipitate were resuspended in 100 μL of Tris-HCl 1 × with 0.2% w/v PEG and 0.05% w/v Tween20. The conjugated AuNPs were stored at 4 °C for further experiments.

### 2.5. Measurement of SARS-CoV-2 pseudovirus without AuNP enhancement using the homemade 96-well chip plate device

The dynamic interaction kinetics of the SARS-CoV-2 pseudovirus particles binding to the immobilized SARS-CoV-2 mAbs with respect to time was performed using the generic microplate reader with our homemade chip-in-microwell plate. 100 μL of different concentrations of pseudovirus particles (covering the range of $10^6$ vp/mL to $10^{10}$ vp/mL) were added to each individual well of the functionalized chip-in-microwell plate. The dynamic absorption spectrum corves were measured using a simple small volume microplate reader (Xlement SPR100, Liangzhun Industrial Co. Ltd, Shanghai, China.) at the specific wavelength 640 nm.

### 2.6. Measurement of SARS-CoV-2 pseudovirus using the AuNP-enhanced techniques

The principle of AuNP-enhanced technique was based on the different antibodies or proteins which could bind to the different epitopes in the receptor-binding domain (RBD) of the SARS-CoV-2 spike protein. In detail, we firstly mixed 30 μL of different concentrations of SARS-CoV-2 pseudovirus with 10 μL of gold labeled ACE2 protein or SARS-CoV-2 mAbs solution, which was followed by dropping the sample mixture into the each well of the sensor chip integrated microwell plate for detection via a generic microplate reader at the specific wavelength 640 nm.

## 3. Results and discussion

### 3.1. Fabrication of nanoplasmonic resonance sensor chip

The purpose of this study is to develop a nanoplasmonic sensor chip detecting SARS-CoV-2 virus particles and controlling the severe pandemic. After the replica molding process as described in the experiment section, the periodic nanocup array sensor chip was fabricated on a polymer substrate with 220 nm nanocup diameter, 500 nm depth and 440 nm periodicity and 70 nm-in-thickness Au layer on it. A high uniformity cup array structure can be seen in the scanning electron microscope (SEM) image of the sensor chip and each nanocup has the similar morphology (Fig. 1b). In addition, media with different refractive index (RI), such as air (RI = 1.0) and water (RI = 1.3), on the sensor chip surface will present distinct colors, which indicates that the sensor chip has highly sensitive with a large spectral change in response to media alterations (Fig. 1b)..(Dang et al., 2019)

### 3.2. Detection principle and technology of nanoplasmonic resonance sensor

The detection technique of one-step rapid quantification of the SARS-CoV-2 pseudovirus was based on a label-free LSPR biosensor with extraordinary optical transmission (EOT) effect(Ebbesen et al., 1998; Hu et al., 2018; Jiang et al., 2018). EOT phenomenon is attributed to the strong field-enhanced plasma excitation in the vicinity of the nanoarrays induced by grating coupling of light at normal incidence illumination, which can simplify optical systems design and generate a high sensitivity to minute local refractive index changes(Ebbesen et al., 1998; Najiminaini et al., 2012). Based on the advantage of EOT, a low-cost ultrasensitive biosensor was integrated into the standard 96-well plate and chip cartridge for direct monitoring the dynamic binding curves of SARS-CoV-2 pseudovirus and SARS-CoV-2 mAbs only using a generic microplate reader and a low-cost handheld optical equipment controlled by a smartphone App (Figure S1, Supporting Information). In addition, previous results indicated that gold nanoparticles (Au-NPs) could significantly enhance the detection sensitivity of the nanoplasmonic biosensor(Belushkin et al., 2018; Seo et al., 2016). The coupling between nanoplasmonic substrates and AuNPs enables quantification of low concentration analyte in a solution with limited diffusion condition. Importantly, AuNP-enhanced technique can further amplify the optical signal and shorten the detection time.

### 3.3. Quantitative determination and specificity verification of SARS-CoV-2 pseudovirus

The quantification of SARS-CoV-2 pseudovirus was measured using standard qRT-PCR method (Lenti-X qRT-PCR Titration Kit, Takara Bio Inc.). The initial concentration after centrifugation of SARS-CoV-2 pseudovirus was determined to be 3.74 × $10^{10}$ vp/mL. Meanwhile, the luciferase activity study showed that the relative luciferase units (RLU.) of the SARS-CoV-2 pseudovirus titration in the pseudovirus infected ACE2-293T cells, which suggesting that the SARS-CoV-2

pseudovirus were successfully constructed and packaged (Figure S2, Supporting Information). In addition, previous studies found that the ACE2 receptor plays a key role in the SARS-CoV-2 pseudovirus interaction with human cells (Wrapp et al., 2020). To further verify the specificity of SARS-CoV-2 pseudovirus, different concentrations of ACE2-mFc proteins was used to block SARS-CoV-2 pseudovirus' infection with ACE2-293T cells (Figure S3, Supporting Information), which is instructive for the development of our specific detection techniques.

### 3.4. Measurement of SARS-CoV-2 pseudovirus using the generic microplate readers with homemade 96-well chip plate device

Fast and sensitive detection of intact coronavirus directly in body fluid samples are essential to diagnose these viruses and help proper treatment. For this reason, our chip-in-microwell sensor were developed for the direct multichannel detection of different concentrations of whole virus particles rather than genetic extraction and analysis methods, which are accurate, but also time-consuming and labor-intensive (Fig. 2a). The surface of the nanoplasmonic array sensor chip was functionalized with SARS-CoV-2-specific antibodies to capture intact coronavirus by binding with spike proteins on its surface (Fig. 2b). The original absorption spectra and differential spectra of adjacent sensor modification steps exhibited obvious change (Fig. 2b and c). From the absorption spectra of the nanocup array chip, the specific resonant wavelength could be seen at 640 nm. In the following experiments, we choose 640 nm to investigate the dynamic binding curves and standard curves with respect to the different concentration of SARS-CoV-2 pseudovirus.

To validate the performance of the homemade 96-well chip plate device, different dilutions of SARS-CoV-2 pseudovirus in PBS solution (from 0 to $1.6 \times 10^{10}$ vp/mL) were added into each well of the 96-well chip plate at the same time. The PBS solution in the absence of SARS-CoV-2 pseudovirus was treated as the control blank group. The real-time dynamic binding curves of the antigen-antibody interaction was shown in Fig. 3a. It can be seen that the curve of the control PBS solution group shows almost no change. Interestingly, the relative OD changes are proportional to the SARS-CoV-2 pseudovirus concentrations. The standard curve of the SARS-CoV-2 pseudovirus detection by the chip-in-microwell sensor over the range of 0–$1.6 \times 10^{10}$ vp/mL is shown in Fig. 3b. The relative OD change value was obtained from the dynamic measurement over 60 min process as shown in Fig. 3a. The results were analyzed and fitted using a four-parameter logistic (4 PL) equation, and the correlation coefficient ($R^2$) is 0.993. Moreover, the $R^2$ is 1.000 in the relatively low virus concentrations range from the 0 to $2.5 \times 10^8$ vp/mL.

In addition, we present a gold nanoparticles (AuNP)-enhanced detection techniques based on our nanoplasmonic resonance sensor device that enables enhanced-sensitivity, rapid and convenience coronavirus detection (Fig. 3c and d). We implemented the proposed techniques for detection of SARS-CoV-2 pseudovirus using the specific binding of SARS-CoV-2 mAbs on the sensor surface and AuNP-labeled ACE2 protein to the different epitopes of the receptor-binding domain (RBD) in SARS-CoV-2 spike protein, respectively. We firstly mixed 30 μL of different concentrations of SARS-CoV-2 pseudovirus with 10 μL of ACE2 protein labeled AuNP solution, and then dropped the sample mixture onto the spike protein specific nanoplasmonic resonance sensor for detection by using a generic microplate reader. The real-time dynamic binding curve of the interaction is represented in Fig. 3e. There is a clear distinction between different concentrations of SARS-CoV-2 pseudovirus within 5 min. Rapid quantitative detection of SARS-CoV-2 virus particles of a much lower concentration range ( from 0 to $6.0 \times 10^5$ vp/mL) was achieved via a single-step AuNP-enhanced nanoplasmonic detection techniques based on our homemade 96-well biosensor chip plate device. The typical differential spectra with different concentrations of SARS-CoV-2 pseudovirus at 10 min was shown in Fig. 4 (Supporting Information). In addition, the 4 PL curve fitting $R^2$ between the relative OD change value and the concentrations of SARS-CoV-2 pseudovirus is 0.985 over the range of 0–$6.0 \times 10^5$ vp/mL, and the $R^2$ is improved up to 1.000 in the lower concentration range

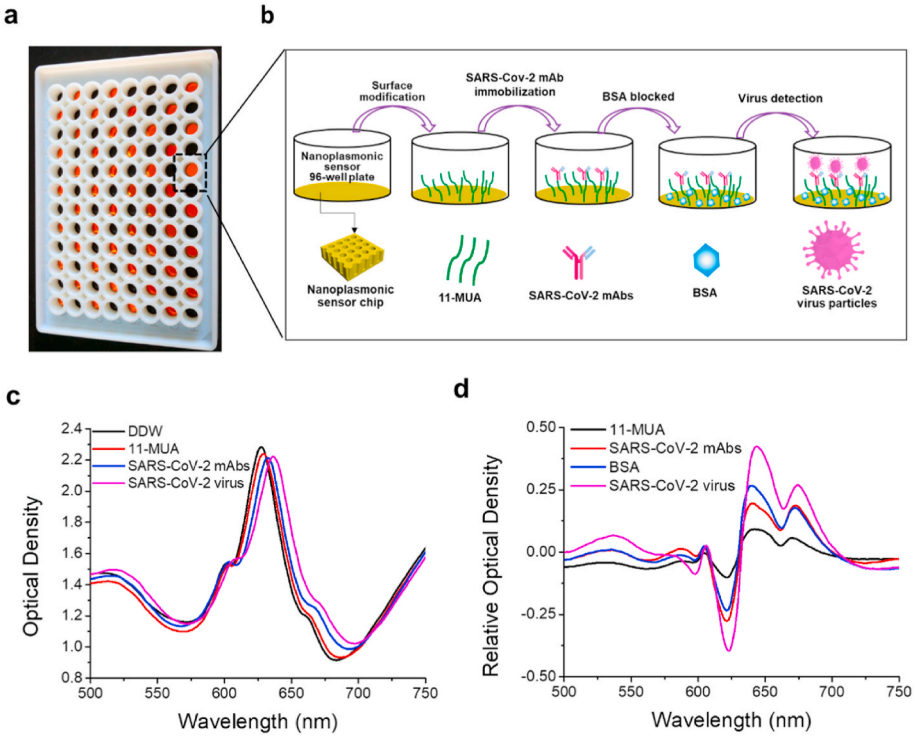


**Fig. 2.** Surface functionalization of nanoplasmonic sensor chip in microwell plate for detecting SARS-CoV-2 virus. (a) Integration of the nanoplasmonic sensor chip with a standard 96-well plate. (b) Schematic of nanoplasmonic sensor chip surface functionalization as well as capturing and detecting SARS-CoV-2 pseudovirus. (c, d) The typical original spectra (c) and differential spectra (d) of adjacent modification steps and detection process with $2.5 \times 10^8$ vp/mL SARS-CoV-2 pseudovirus.

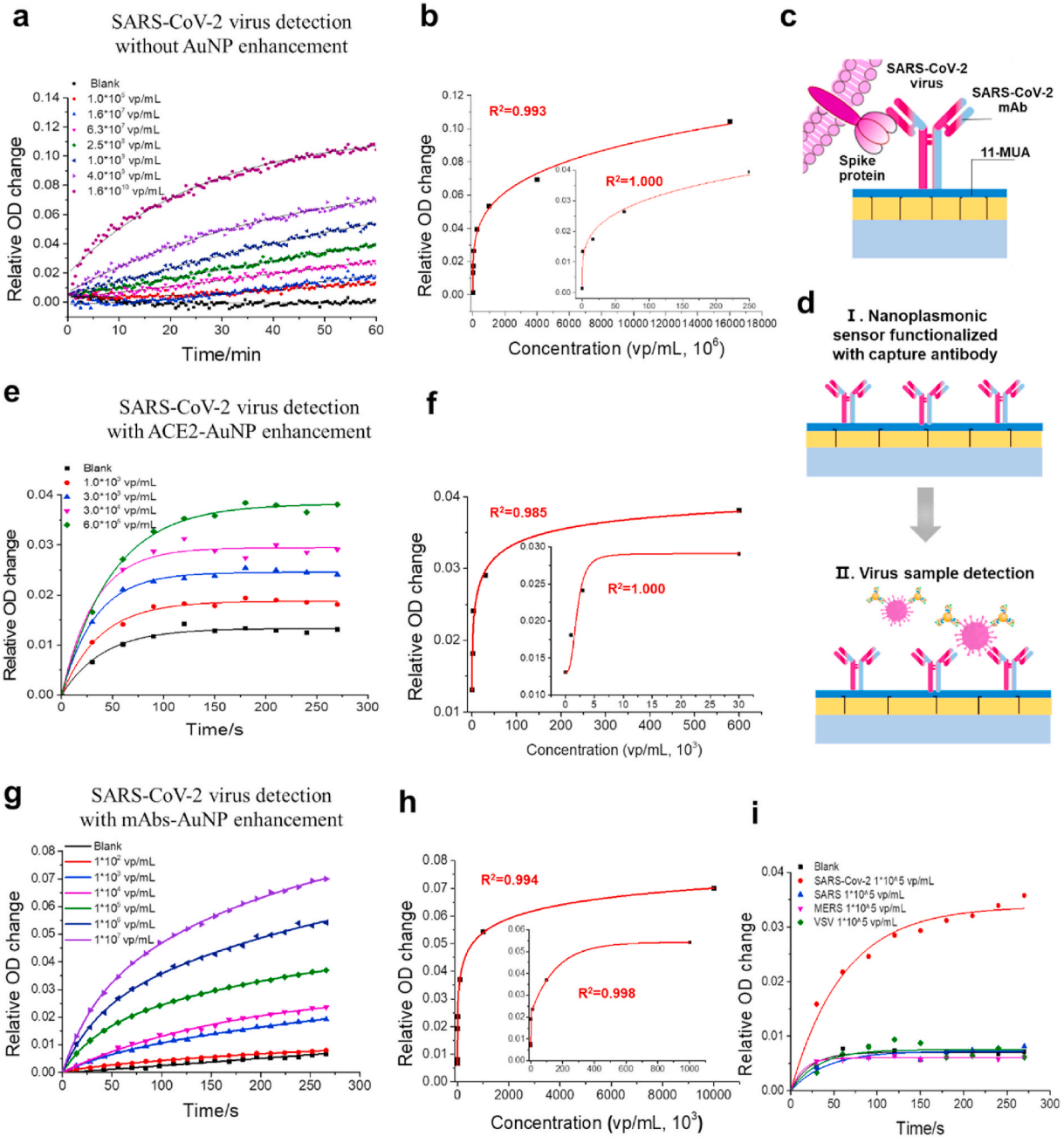


**Fig. 3.** Detection of SARS-CoV-2 pseudovirus with nanoplasmonic sensor chip by a generic microplate reader. (a) Dynamic binding curves of SARS-CoV-2 antibodies interaction with different concentrations of the SARS-CoV-2 pseudovirus over the range 0–1.6 × $10^{10}$ vp/mL at the resonant wavelength. (b) SARS-CoV-2 pseudovirus standard curve ($R^2 = 0.993$). (c) The illustration shows the binding of spike protein on the surface of SARS-CoV-2 virus to the specific SARS-CoV-2 mAbs. SARS-CoV-2 antibodies are conjugated to the activated carboxyl groups of 11-MUA on chip surface. (d) Schematic of nanoplasmonic sensor chip detecting SARS-CoV-2 pseudovirus with AuNP enhancement. (e) ACE2 protein labeled AuNP enhanced binding curves with different concentrations of the SARS-CoV-2 pseudovirus over the range 0–6.0 × $10^5$ vp/mL. (f) ACE2 protein labeled AuNP enhanced SARS-CoV-2 pseudovirus standard curve ($R^2 = 0.985$). (g) SARS-CoV-2 mAbs labeled AuNP enhanced binding curves with different concentrations of the SARS-CoV-2 pseudovirus over the range 0–1.0 × $10^7$ vp/mL. (h) SARS-CoV-2 mAbs labeled AuNP enhanced SARS-CoV-2 pseudovirus standard curve ($R^2 = 0.994$). (i) Specificity verification test of AuNP-enhanced SARS-CoV-2 pseudovirus detection: Dynamic binding curves of SARS-CoV-2 antibodies interaction with different pseudovirus of SARS-CoV-2, SARS, MERS, and VSV at the concentration of 1.0 × $10^5$ vp/mL.

from 0 to 3.0 × $10^4$ vp/mL (Fig. 3f).

Human ACE2 protein could bind to the RBD of S protein in both SARS-CoV-2 and SARS-CoV, which may reduce the specificity and sensitivity of our sensor chip. Therefore, we used paired antibody sandwich detection, that is, one kind of S protein antibodies conjugated on the nanocup sensor surface and another kind of S protein antibodies labeled on the AuNP surface to respectively capture two distinctive epitopes of the S proteins on the viral particle surface. As expected, the single-step double-antibody sandwich plasmonic resonance immunoassay method can not only expand the detection range (0–1.0 × $10^7$ vp/mL), but also improve the detection specificity (Fig. 3g–i). In addition, the results were fit to the 4 PL curve and showed good agreement over the range of 0–1.0 × $10^7$ vp/mL, the coefficient of determination ($R^2$) for fitting was found to be 0.994, and the fitting equation is $y = 0.093 + [1 + (x/829.33)^{-0.318}] + 0.006$ (Fig. 3h). Similarly, the $R^2$ also reached 0.998 in the lower concentration range from 0 to 1.0 × $10^6$ vp/mL (Fig. 3h). The theoretical limit of detection (LOD) of this double-antibody sandwich method was reduced to about 370 vp/

mL. Notably, the typical viral concentration is at a wide range from $10^4$–$10^{10}$ vp/mL in nasopharyngeal swab and saliva (Azzi et al., 2020; Williams et al., 2020; Wyllie et al., 2020; Yoon et al., 2020), suggesting that the chip-in-microwell sensor has the potential to detect SARS-CoV-2 virus with an ultrahigh sensitivity and effectiveness in early infection diagnostics, compared to existing technologies requiring laborious sample processing and time-consuming detection.

Reliable detection of SARS-CoV-2 virus requires distinguishing nonspecific binding of other viruses to the functionalized nanoplasmonic sensor surface. Virus selectivity is achieved by surface immobilized highly specific antibodies CR3022 showing strong affinity only to the SARS-CoV-2 coronavirus membrane S proteins (Wang et al., 2020) (Fig. 3c). Here, the detection specificity was evaluated with the SARS, MERS, and VSV in comparison with SARS-CoV-2 pseudovirus. A significant difference in binding capacity was observed with a high response to the SARS-CoV-2 viruses while almost no response to other virus strains (Fig. 3i, Figure S5-7, Supporting Information) These results demonstrate that the functionalized nanoplasmonic sensor chip has very high specificity in detecting the SARS-CoV-2 virus.

### 3.5. *Measurement of SARS-CoV-2 pseudovirus using a low-cost handheld optical equipment controlled by a smartphone App*

Demand for rapid, accurate and convenient SARS-CoV-2 virus detection present significant challenges in controlling and stopping the pandemics. Diagnosis of patients in the early stage infection are so far limited to viral nucleic acid or antigen detection in human nasopharyngeal swabs or saliva samples. Although traditional approaches, including point-of-care (POC) diagnostics, bedside testing, and community-based approaches, were applied to address these challenges, innovative techniques combining with mobile technologies, nanotechnology, imaging systems, and microfluidic technologies are expected to promote this transformation (Im et al., 2014; Li et al., 2017; Wang et al., 2017). In this work, we also developed a portable and innovative devices controlled by a smartphone App for real-time measurements of the dynamic binding curves of SARS-CoV-2 virus on the nanoplasmonic sensor (Fig. 4a). We integrated the nanoplasmonic sensor chip in a cartridge designed for the handheld testing device, followed by functional modification of the sensor chip and detection of pseudovirus particle samples according to the protocol described previously (Fig. 4b). The functionalized chip cartridge with different concentrations of pseudovirus samples was inserted into the testing device and the dynamic curves were recorded in real time through the smartphone APP. The real-time virus binding curve measurement is presented in Fig. 4c and Video 1. This low-cost handheld sensing platform can directly detect the SARS-CoV-2 pseudovirus sample in one step within 15 min and the detectable virus concentrations range over 0 to 6.0 × $10^6$ vp/mL. Moreover, the quantification limit of the handheld equipment is currently about 4000 SARS-CoV-2 virus particles and can be further improved to be comparable with the microplate reader case.

Supplementary video related to this article can be found at https://doi.org/10.1016/j.bios.2020.112685

Furthermore, the detection specificity of the handheld devices for SARS-CoV-2 pseudovirus was also characterized with the SARS, MERS, and VSV pseudovirus. As shown in Fig. 4d, there was no obvious change in the curves of SARS, MERS, and VSV pseudovirus. A remarkably rising curve was observed only for the SARS-CoV-2 pseudovirus sample, suggesting that the devices controlled by a smartphone App could offer convenient operability while permit highly sensitive and specific detection of SARS-CoV-2 pseudovirus. This nanoplasmonic sensor device with the potential in rapid and affordable early diagnosis of COVID-19 disease will become available for POC applications in clinics, roadside triage site and even home settings.

## 4. Conclusion

At present the COVID-19 pandemic is still affecting the whole world. However, there are just a limited rapid diagnostic methods or testing equipments that are effective for newly infected patients or asymptomatic carriers. In addition, most detection methods for SARS-CoV-2 viruses have high logistical barriers and thus are not suitable for POC testing. Therefore in this work, we developed a simple and low-cost device to rapidly and sensitively detect the SARS-CoV-2 virus in one step using a nanoplasmonic biosensor integrated with a standard 96-well plate or a chip cartridge. Our study confirmed that the nanoplasmonic sensor chip is able to directly detect the whole SARS-CoV-2 virus with extraordinary time efficiency (<15 min) and sensitivity (LOD = 370 vp/mL). Moreover, similar rapid and sensitive detection

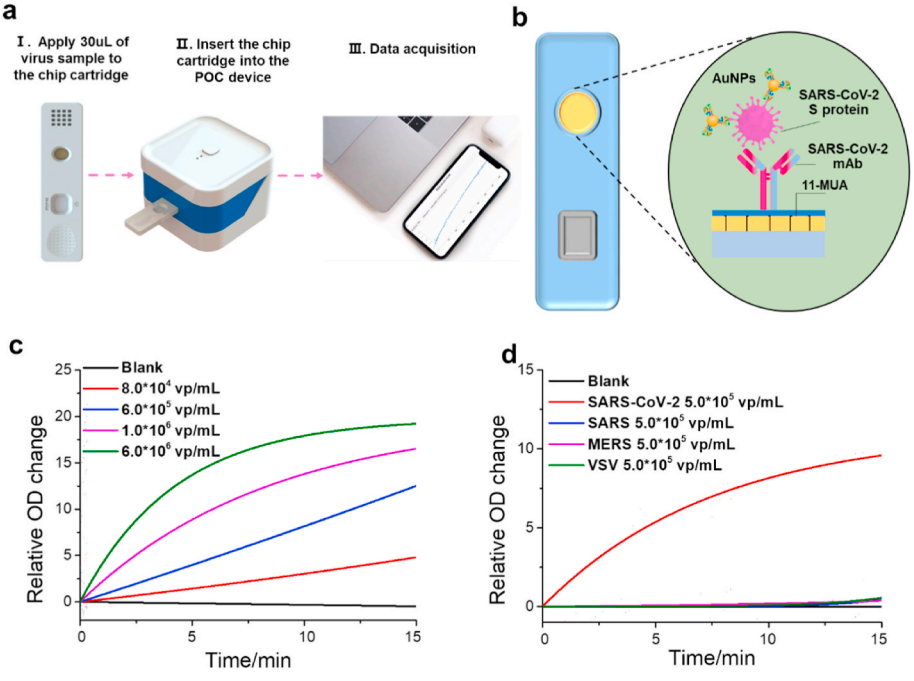


**Fig. 4.** Detection of SARS-CoV-2 pseudovirus with nanoplasmonic sensor chips by a point-of-care device. (a) Schematic of nanoplasmonic sensor chip cartridge detecting SARS-CoV-2 pseudovirus with a low-cost handheld point-of-care testing device. (b) The illustration shows the detection process of the sensor chip cartridge for specific SARS-CoV-2 detection. (c) Dynamic binding curves of virus and antibody interaction with different concentrations of the SARS-CoV-2 pseudovirus over the range 0–6.0 × $10^6$ vp/mL at the resonance wavelength. (d) Specificity verification test: Dynamic binding curves of SARS-CoV-2 antibodies interaction with different pseudovirus of SARS-CoV-2, SARS, MERS, and VSV at the concentration of 5.0 × $10^5$ vp/mL.

capabilities are demonstrated by using a low-cost handheld optical equipment controlled by a smartphone App. The quantification limit of SARS-CoV-2 pseudovirus in the handheld system was about 4000 virus particles within 15 min. We therefore conclude that the low-cost POCT devices would be expected for rapid diagnosis of SARS-CoV-2 virus infection.

## CRediT authorship contribution statement

**Liping Huang:** Conceptualization, Methodology, Investigation, Data curation, Visualization, Writing - original draft. **Longfei Ding:** Pseudovirus production and quantification. **Jun Zhou:** Chip manufacturing, Pseudovirus design and antibody selection. **Shuiliang Chen:** Chip manufacturing. **Fang Chen:** Chip manufacturing. **Chen Zhao:** Investigation, Resources. **Jianqing Xu:** Medical advisory. **Wenjun Hu:** Supervision, Funding acquisition. **Jiansong Ji:** Supervision, Writing - review & editing, Project administration.

## Declaration of competing interest

The authors declare that they have no known competing financial interests or personal relationships that could have appeared to influence the work reported in this paper.

## Acknowledgments

This work was supported by National Natural Science Foundation of China (91959107). Fundamental Research Funds for the Central Universities (2020kfyXGYJ111). The authors thank Lu Wang, Hong Yang and Hui Guo for their help with data acquisition.

## Appendix A. Supplementary data

Supplementary data related to this article can be found at https://doi.org/10.1016/j.bios.2020.112685.

## References

Ai, J.-W., Zhang, H.-C., Xu, T., Wu, J., Zhu, M., Yu, Y.-Q., Zhang, H.-Y., Shen, Z., Li, Y., Zhou, X., Zang, G.-Q., Xu, J., Chen, W.-J., Li, Y.-J., Xie, D.-S., Zhou, M.-Z., Sun, J.-Y., Chen, J.-Z., Zhang, W.-H., 2020. Optimizing diagnostic strategy for novel coronavirus pneumonia, a multi-center study in Eastern China. medRxiv 2020, 2002.2013.20022673.

Azzi, L., Carcano, G., Gianfagna, F., Grossi, P., Gasperina, D.D., Genoni, A., Fasano, M., Sessa, F., Tettamanti, L., Carinci, F., Maurino, V., Rossi, A., Tagliabue, A., Baj, A., 2020. Saliva is a reliable tool to detect SARS-CoV-2. J. Infect. 81, e45–e50.

Baek, Y.H., Um, J., Antigua, K.J.C., Park, J.H., Kim, Y., Oh, S., Kim, Y.I., Choi, W.S., Kim, S.G., Jeong, J.H., Chin, B.S., Nicolas, H.D.G., Ahn, J.Y., Shin, K.S., Choi, Y.K., Park, J.S., Song, M.S., 2020. Development of a reverse transcription-loop-mediated isothermal amplification as a rapid early-detection method for novel SARS-CoV-2. Emerg. Microb. Infect. 9 (1), 998–1007.

Belushkin, A., Yesilkoy, F., Altug, H., 2018. Nanoparticle-enhanced plasmonic biosensor for digital biomarker detection in a microarray. ACS Nano 12 (5), 4453–4461.

Chang, Y.F., Wang, W.H., Hong, Y.W., Yuan, R.Y., Chen, K.H., Huang, Y.W., Lu, P.L., Chen, Y.H., Chen, Y.A., Su, L.C., Wang, S.F., 2018. Simple strategy for rapid and sensitive detection of avian influenza A H7N9 virus based on intensity-modulated SPR biosensor and new generated antibody. Anal. Chem. 90 (3), 1861–1869.

Chen, Z., Zhang, Z., Zhai, X., Li, Y., Lin, L., Zhao, H., Bian, L., Li, P., Yu, L., Wu, Y., Lin, G., 2020. Rapid and sensitive detection of anti-SARS-CoV-2 IgG, using lanthanide-doped nanoparticles-based lateral flow immunoassay. Anal. Chem. 92 (10), 7226–7231.

Corman, V.M., Landt, O., Kaiser, M., Molenkamp, R., Meijer, A., Chu, D.K.W., Bleicker, T., Brunink, S., Schneider, J., Schmidt, M.L., Mulders, D.G.J.C., Haagmans, B.L., van der Veer, B., van den Brink, S., Wijsman, L., Goderski, G., Romette, J.L., Ellis, J., Zambon, M., Peiris, M., Goossens, H., Reusken, C., Koopmans, M.P.G., Drosten, C., 2020. Detection of 2019 novel coronavirus (2019-nCoV) by real-time RT-PCR. Euro Surveill. 25 (3), 23–30.

Dang, T., Hu, W., Zhang, W., Song, Z., Wang, Y., Chen, M., Xu, H., Liu, G.L., 2019. Protein binding kinetics quantification via coupled plasmonic-photonic resonance nanosensors in generic microplate reader. Biosens. Bioelectron. 142, 111494.

Ebbesen, T.W., Lezec, H.J., Ghaemi, H.F., Thio, T., Wolff, P.A., 1998. Extraordinary optical transmission through sub-wavelength hole arrays. Nature 391 (6668), 667–669.

Guan, M., Chen, H.Y., Foo, S.Y., Tan, Y.J., Goh, P.Y., Wee, S.H., 2004. Recombinant protein-based enzyme-linked immunosorbent assay and immunochromatographic tests for detection of immunoglobulin G antibodies to severe acute respiratory syndrome (SARS) coronavirus in SARS patients. Clin. Diagn. Lab. Immunol. 11 (2), 287–291.

Haveri, A., Smura, T., Kuivanen, S., Österlund, P., Hepojoki, J., Ikonen, N., Pitkäpaasi, M., Blomqvist, S., Rönkkö, E., Kantele, A., Strandin, T., Kallio-Kokko, H., Mannonen, L., Lappalainen, M., Broas, M., Jiang, M., Siira, L., Salminen, M., Puumalainen, T., Sane, J., Melin, M., Vapalahti, O., Savolainen-Kopra, C., 2020. Serological and molecular findings during SARS-CoV-2 infection: the first case study in Finland, January to February 2020. Euro Surveil.: bulletin Europeen sur les maladies transmissibles = European communicable disease bulletin 25 (11).

Hoffmann, M., Kleine-Weber, H., Schroeder, S., Kruger, N., Herrler, T., Erichsen, S., Schiergens, T.S., Herrler, G., Wu, N.H., Nitsche, A., Muller, M.A., Drosten, C., Pohlmann, S., 2020. SARS-CoV-2 cell entry depends on ACE2 and TMPRSS2 and is blocked by a clinically proven protease inhibitor. Cell 181 (2), 271–280 e278.

Hu, W., Dang, T., Li, Z., Lei, L., Wang, G., Li, Y., Xu, H., Zhou, Z., Liu, G.L., 2019. C-reaction protein detection in human saliva by nanoplasmonic color imaging. J. Biomed. Nanotechnol. 15 (8), 1724–1733.

Hu, Y., Ameen, A., Hsiao, A., Liu, G.L., 2018. Colorimetric imaging of layer-by-layer molecular deposition on nanoplasmonic lycurgus cup array. Sensor. Actuator. 254, 827–833.

Im, H., Shao, H., Park, Y.I., Peterson, V.M., Castro, C.M., Weissleder, R., Lee, H., 2014. Label-free detection and molecular profiling of exosomes with a nano-plasmonic sensor. Nat. Biotechnol. 32 (5), 490–495.

Jackman, J.A., Linardy, E., Yoo, D., Seo, J., Ng, W.B., Klemme, D.J., Wittenberg, N.J., Oh, S.H., Cho, N.J., 2016. Plasmonic nanohole sensor for capturing single virus-like particles toward virucidal drug evaluation. Small 12 (9), 1159–1166.

Jiang, J., Wang, X., Li, S., Ding, F., Li, N., Meng, S., Li, R., Qi, J., Liu, Q., Liu, G.L., 2018. Plasmonic nano-arrays for ultrasensitive bio-sensing. Nanophotonics 7 (9), 1517–1531.

Li, X., Soler, M., Ozdemir, C.I., Belushkin, A., Yesilkoy, F., Altug, H., 2017. Plasmonic nanohole array biosensor for label-free and real-time analysis of live cell secretion. Lab Chip 17 (13), 2208–2217.

Lipman, M., Chambers, R.C., Singer, M., Brown, J.S., 2020. SARS-CoV-2 Pandemic: Clinical Picture of COVID-19 and Implications for Research. Thorax thoraxjnl-2020-215024.

Liu, L., Liu, W., Zheng, Y., Jiang, X., Kou, G., Ding, J., Wang, Q., Huang, Q., Ding, Y., Ni, W., Wu, W., Tang, S., Tan, L., Hu, Z., Xu, W., Zhang, Y., Zhang, B., Tang, Z., Zhang, X., Li, H., Rao, Z., Jiang, H., Ren, X., Wang, S., Zheng, S., 2020. A preliminary study on serological assay for severe acute respiratory syndrome coronavirus 2 (SARS-CoV-2) in 238 admitted hospital patients. Microb. Infect. 22 (4–5), 206–211.

Loeffelholz, M.J., Tang, Y.W., 2020. Laboratory diagnosis of emerging human coronavirus infections - the state of the art. Emerg. Microb. Infect. 9 (1), 747–756.

Lu, R., Wu, X., Wan, Z., Li, Y., Jin, X., Zhang, C., 2020. A novel reverse transcription loop-mediated isothermal amplification method for rapid detection of SARS-CoV-2. Int. J. Mol. Sci. 21 (8).

Moran, K.L.M., Lemass, D., O'Kennedy, R., 2018. Surface Plasmon Resonance–Based Immunoassays, pp. 129–156.

Najiminaini, M., Vasefi, F., Kaminska, B., Carson, J.J.L., 2012. Nano-hole array structure with improved surface plasmon energy matching characteristics. Appl. Phys. Lett. 100 (4), 043105.

Puiu, M., Bala, C., 2016. SPR and SPR imaging: recent trends in developing nanodevices for detection and real-time monitoring of biomolecular events. Sensors 16 (6), 870.

Rabaan, A., Al-Ahmed, S., Haque, S., Sah, R., Tiwari, R., Malik, Y., Dhama, K., Yatoo, D. M., Bonilla-Aldana, D., Rodriguez-Morales, A., 2020. SARS-CoV-2, SARS-CoV, and MERS-CoV: a comparative overview. Le infezioni in medicina: rivista periodica di eziologia, epidemiologia, diagnostica, clinica e terapia delle patologie infettive, vol. 28, pp. 174–184.

Seo, S., Zhou, X., Liu, G.L., 2016. Sensitivity tuning through additive heterogeneous plasmon coupling between 3D assembled plasmonic nanoparticle and nanocup arrays. Small 12 (25), 3453–3462.

Sethuraman, N., Jeremiah, S.S., Ryo, A., 2020. Interpreting diagnostic tests for SARS-CoV-2. J. Am. Med. Assoc. 323 (22), 2249–2251.

Soler, M., Belushkin, A., Cavallini, A., Kebbi-Beghdadi, C., Greub, G., Altug, H., 2017. Multiplexed nanoplasmonic biosensor for one-step simultaneous detection of Chlamydia trachomatis and Neisseria gonorrhoeae in urine. Biosens. Bioelectron. 94, 560–567.

Su, L.C., Chang, C.M., Tseng, Y.L., Chang, Y.F., Li, Y.C., Chang, Y.S., Chou, C., 2012. Rapid and highly sensitive method for influenza A (H1N1) virus detection. Anal. Chem. 84 (9), 3914–3920.

To, K.K., Tsang, O.T., Leung, W.S., Tam, A.R., Wu, T.C., Lung, D.C., Yip, C.C., Cai, J.P., Chan, J.M., Chik, T.S., Lau, D.P., Choi, C.Y., Chen, L.L., Chan, W.M., Chan, K.H., Ip, J.D., Ng, A.C., Poon, R.W., Luo, C.T., Cheng, V.C., Chan, J.F., Hung, I.F., Chen, Z., Chen, H., Yuen, K.Y., 2020. Temporal profiles of viral load in posterior oropharyngeal saliva samples and serum antibody responses during infection by SARS-CoV-2: an observational cohort study. Lancet Infect. Dis. 20 (5), 565–574.

Victoria, S., 2012. Application of surface plasmon resonance (SPR) for the detection of single viruses and single biological nano-objects. J. Bacteriol. Parasitol. 3 (7).

Wang, C., Li, W., Drabek, D., Okba, N.M.A., van Haperen, R., Osterhaus, A., van Kuppeveld, F.J.M., Haagmans, B.L., Grosveld, F., Bosch, B.J., 2020. A human monoclonal antibody blocking SARS-CoV-2 infection. Nat. Commun. 11 (1), 2251.

Wang, X., Chang, T.W., Lin, G., Gartia, M.R., Liu, G.L., 2017. Self-referenced smartphone-based nanoplasmonic imaging platform for colorimetric biochemical sensing. Anal. Chem. 89 (1), 611–615.

Wang, Y., Cui, D., Wang, J., Cai, H., Zheng, Z., Deng, W., Qin, C., Yang, X., 2006. The Detection of SARS-CoV with SPR Biosensor.
Williams, E., Bond, K., Zhang, B., Putland, M., Williamson, D.A., 2020. Saliva as a non-invasive specimen for detection of SARS-CoV-2. J. Clin. Microbiol. 58 (8).
Wrapp, D., Wang, N., Corbett, K.S., Goldsmith, J.A., Hsieh, C.-L., Abiona, O., Graham, B. S., McLellan, J.S., 2020. Cryo-EM structure of the 2019-nCoV spike in the prefusion conformation. Science 367 (6483), 1260–1263.
Wyllie, A., Fournier, J., Casanovas-Massana, A., Campbell, M., Tokuyama, M., Vijayakumar, P., Geng, B., Muenker, M., Moore, A., Vogels, C., Petrone, M., Ott, I., Lu, P., Venkataraman, A., Lu-Culligan, A., Klein, J., Earnest, R., Simonov, M., Datta, R., Ko, A., 2020. Saliva Is More Sensitive for SARS-CoV-2 Detection in COVID-19 Patients than Nasopharyngeal Swabs.
Yan, C., Cui, J., Huang, L., Du, B., Chen, L., Xue, G., Li, S., Zhang, W., Zhao, L., Sun, Y., Yao, H., Li, N., Zhao, H., Feng, Y., Liu, S., Zhang, Q., Liu, D., Yuan, J., 2020. Rapid and visual detection of 2019 novel coronavirus (SARS-CoV-2) by a reverse transcription loop-mediated isothermal amplification assay. Clinical microbiology and infection : the official publication of the European Society of Clinical Microbiology and Infectious Diseases 26 (6), 773–779.
Yang, Y., Lu, Q., Liu, M., Wang, Y., Zhang, A., Jalali, N., Dean, N., Longini, I., Halloran, M.E., Xu, B., Zhang, X., Wang, L., Liu, W., Fang, L., 2020. Epidemiological and clinical features of the 2019 novel coronavirus outbreak in China. medRxiv 2020, 2002.2010.20021675.
Yanik, A.A., Huang, M., Kamohara, O., Artar, A., Geisbert, T.W., Connor, J.H., Altug, H., 2010. An optofluidic nanoplasmonic biosensor for direct detection of live viruses from biological media. Nano Lett. 10 (12), 4962–4969.
Yoon, J.G., Yoon, J., Song, J.Y., Yoon, S.Y., Lim, C.S., Seong, H., Noh, J.Y., Cheong, H.J., Kim, W.J., 2020. Clinical significance of a high SARS-CoV-2 viral load in the saliva. J. Kor. Med. Sci. 35 (20), e195.
Younes, N., Al-Sadeq, D.W., Al-Jighefee, H., Younes, S., Al-Jamal, O., Daas, H.I., Yassine, H.M., Nasrallah, G.K., 2020. Challenges in laboratory diagnosis of the novel coronavirus SARS-CoV-2. Viruses 12 (6).
Zhang, D., Zhang, Q., Lu, Y., Yao, Y., Li, S., Jiang, J., Liu, G.L., Liu, Q., 2016. Peptide functionalized nanoplasmonic sensor for explosive detection. Nano-Micro Lett. 8 (1), 36–43.